Eurasian Chem.-Technol. J. 28 (2026) 117–126
The journal of the Institute of Combustion Problems https://ect-journal.kz

https://doi.org/10.18321/ectj1688

Hydrogen Fluoride Formation During Slow Reaction and Auto-Ignition Processes of Stoichiometric R32-Air Mixtures

Chunkan Yu* and Ulrich Maas

Institute of Technical Thermodynamics, Karlsruhe Institute of Technology, Karlsruhe, Germany

Article info

Received:
16 January 2026

Received in revised form:
3 April 2026

Accepted:
18 May 2026

Keywords:
Refrigerant; R32-oxygen mixture; Explosion limit; Auto-ignition; Process safety

Abstract

The formation of hydrogen fluoride (HF) during the auto-ignition process of stoichiometric difluoromethane (R32)-air mixtures is numerically investigated in a cylindrical vessel under the influence of heat losses and heterogeneous wall reactions. Both slow reaction and successful explosion regimes are analyzed to study the thermo-kinetic conditions leading to HF formation. A detailed chemical mechanism is used for the gas-phase chemistry, while heterogeneous destruction reactions of reactive species at the wall surface are additionally considered. The effects of initial temperature, pressure and surface destruction efficiencies on HF production are investigated. Particular attention is paid to the role of OH radicals and heterogeneous wall reactions in controlling the formation of HF under non-explosive conditions.

1. Introduction

Refrigerants are the key working fluids in air-conditioning and refrigeration systems, where they enable heat transfer and strongly influence the cooling performance, energy efficiency and environmental impact of the system [1–4]. Among the currently available refrigerants, R32 (difluoromethane, CH_2F_2) has attracted increasing attention as a next-generation refrigerant because of its relatively low global warming potential (GWP ≈ 675), which is approximately one third of that of R410A [2, 5, 6]. Owing to this environmental advantage, R32 has been increasingly adopted in Europe, the United States and many other regions as a replacement for R410A in residential air-conditioning systems [6]. In addition, R32 shows favorable thermodynamic properties and a zero-ozone depletion potential (ODP), making it an environmentally attractive refrigerant [1, 5].

Despite these advantages, R32 is classified as a mildly flammable refrigerant [7, 8], requiring additional safety measures during installation and maintenance, such as sufficient ventilation and avoidance of ignition sources. Although the relatively low burning velocity of R32 allows safe operation under properly controlled conditions [9], its combustion and auto-ignition characteristics remain important concerns in process and safety engineering.

Previous studies on R32 combustion mainly focused on flame propagation, burning velocities and quenching process [9–12]. In addition to explosion hazards, the combustion and oxidation of fluorinated refrigerants can also lead to the formation of highly toxic products. In particular, hydrogen fluoride (HF) is considered one of the most hazardous combustion products due to its severe toxicity and corrosive properties. Exposure to HF even at relatively low concentrations may result in serious health risks. In [13], an experimental investigation on the main toxic combustion product, hydrogen fluoride (HF), of R32 was conducted. It was found that the HF concentration can reach up to 80 ppm for the combustion of a 16.9% R32/83.1% O_2 mixture, which may cause serious damage to human health. Therefore, understanding the formation mechanisms and accumulation conditions of HF is essential for the safety assessment of R32-containing systems.

*Corresponding author.
E-mail address: chunkan.yu@kit.edu

While the formation of toxic products is often associated with explosion or intense combustion events, hazardous species may also be generated under slow oxidation or non-explosive conditions. In systems with heat losses and heterogeneous wall effects, the competition between chemical heat release, diffusive transport, and radical destruction at the wall can suppress thermal runaway while still allowing slow chemical reactions to proceed over long periods. Under such conditions, toxic products may accumulate even though no significant temperature rise or explosion is observed. However, the production of HF during non-explosive auto-ignition processes of R32-air mixtures has received only limited attention so far.

In the present work, the auto-ignition process of stoichiometric R32-air mixtures in a cylindrical vessel is investigated numerically with particular focus on HF formation. Heat losses and heterogeneous surface reactions are included in the model in order to account for wall effects on the thermo-kinetic behavior of the system. The study analyzes both slow reaction and successful explosion regimes and investigates the influence of pressure, temperature, and wall destruction efficiencies on HF production. The obtained results provide qualitative insights into the relationship between auto-ignition behavior and toxic product formation in R32-air systems and contribute to the safety assessment of fluorinated refrigerants.

2. Mathematical model

To investigate the HF production, the auto-ignition process is modeled in a cylindrical vessel. Particularly, a pre-mixed gas mixture is initially introduced into the vessel at a high temperature sufficient to initiate auto-ignition. While the temperature of the gas mixture rises during the reaction, the vessel surface is maintained at its initial temperature, constituting a fixed thermal boundary condition (Dirichlet boundary condition). Radicals produced by the chemical reactions can react upon reaching the vessel surface. Both processes introduce two critical effects: heat loss due to a temperature gradient at the surface and the destruction of radicals through heterogeneous surface reactions. Both mechanisms act as suppressants to the auto-ignition process and can prevent the mixture from reaching the conditions necessary for a successful explosion.

While a detailed discussion and derivation of the mathematical formulation for the governing equations of species mass, momentum and energy can be found in [14], this section will provide a concise overview of the most crucial assumptions, transformations and governing equations applied in the present work for better clarity.

2.1. Governing equations with initial and boundary conditions

In general, the auto-ignition process in a cylindrical vessel can be described by the governing equations of species mass, momentum, and energy in cylindrical coordinates assuming a one-dimensional geometry. Following the approach proposed in [14], a Lagrangian coordinate transformation is applied, which eliminates the convective terms from the governing equations. In addition, the continuity equation is automatically satisfied in the transformed coordinate system and therefore does not need to be solved explicitly. Assuming spatially uniform pressure inside the reaction vessel (which is a good assumption for the slowly igniting compound), the governing equations can be written as [14]:

$$\frac{\partial r}{\partial \psi} - \frac{1}{\rho r} = 0 \tag{1}$$

$$\frac{\partial p}{\partial \psi} = 0 \tag{2}$$

$$\frac{\partial w_i}{\partial t} + \frac{\partial}{\partial \psi}(\rho r w_i V_i) - \frac{\dot{\omega}_i M_i}{\rho} = 0 \tag{3}$$

$$\rho c_p \frac{\partial T}{\partial t} - \frac{\partial p}{\partial t} - \rho \frac{\partial}{\partial \psi}\left(\rho r^2 \lambda \frac{\partial T}{\partial \psi}\right) + \rho r^2 \sum_{i=1}^{n_s} \rho w_i V_i c_{p,i} \frac{\partial T}{\partial \psi} + \sum_{i=1}^{n_s} \dot{\omega}_i h_i M_i = 0 \tag{4}$$

Here, r denotes the radius, p the pressure, T the temperature, and ρ the density. Furthermore, c_p and λ represent the isobaric specific heat capacity and thermal conductivity of the gas mixture, respectively. The number of species is denoted by n_s, while w_i, M_i, h_i, and $\dot{\omega}_i$ correspond to the mass fraction, molar mass, specific enthalpy and molar production rate of species i, respectively. The quantity $c_{p,i}$ represents the specific isobaric heat capacity of species i. The diffusion velocity V_i includes both differential diffusion and thermal diffusion (Soret effect) according to [15].

For the initial condition, the fields of reactant concentrations and temperatures are homogeneously distributed as:

$$T(\psi, t=0) = T_0, \quad w_i(\psi, t=0) = w_{i,0} \tag{5}$$

At the center of the reaction vessel (r = 0 or ψ = 0), symmetry boundary conditions are applied:

$$r(\psi = 0, t) = 0, \quad \left.\frac{\partial T}{\partial \psi}\right|_{\psi=0,t} = 0 \quad \left.\frac{\partial w_i}{\partial \psi}\right|_{\psi=0,t} = 0 \tag{6}$$

At the outer boundary condition which is applied at the vessel surface, the temperature is assumed to be constant at T_0 and the total mass flux of species i vanishes at the surface. Thus the corresponding boundary conditions are formulated as:

$$r(\psi = \psi^s, t) = R, \quad T(\psi = \psi^s, t) = T_0, \quad \rho w_i V_i + \dot{\omega}_i^s = 0 \tag{7}$$

where R is the radius of the cylindrical vessel.

2.2. Gas mixture and chemical mechanism

The R32 (CH_2F_2)-air premixed mixture is considered. The stoichiometric mixture is the focus of the present work because the corresponding premixed flame has the highest laminar flame speed [9], which can be regarded as the most critical mixture condition. Investigation of extended fuel/air equivalence ratios is part of our ongoing research. For this mixture the corresponding stoichiometric mixture reads

$$CH_2F_2 : O_2 : N_2 = 1 : 1 : \frac{79}{21}$$

The chemical mechanism used for the numerical simulation was developed at NIST [16] and includes 104 species. This mechanism has been validated for the laminar flame speed of R32/air for a wide range of equivalence ratios between 0.9 and 1.4. It should be noted that, due to the lack of experimental data for shock tube and rapid compression machine (RCM) experiments, the chemical mechanism used in this study has not been validated for ignition delay times. Consequently, uncertainties in the chemistry may affect the predicted reaction progress and therefore the quantitative prediction of HF formation. For this reason, the present work focuses on identifying qualitative trends and dominant formation mechanisms rather than providing quantitatively accurate HF concentrations. Future work will include a quantitative assessment once ignition delay data become available and the chemical mechanism has been validated.

Since the components produced through chemical reactions can also help determine whether an explosion occurred, it is necessary to identify the main products generated under stoichiometric conditions. Therefore, as a reference, the chemical equilibrium composition is calculated for different initial temperatures and pressures under constant-enthalpy conditions corresponding to the initial thermodynamic state. Figure 1 presents the calculated mole fractions of CO_2, HF, CF_2O and H_2O for stoichiometric R32-air mixtures at equilibrium state. It is observed

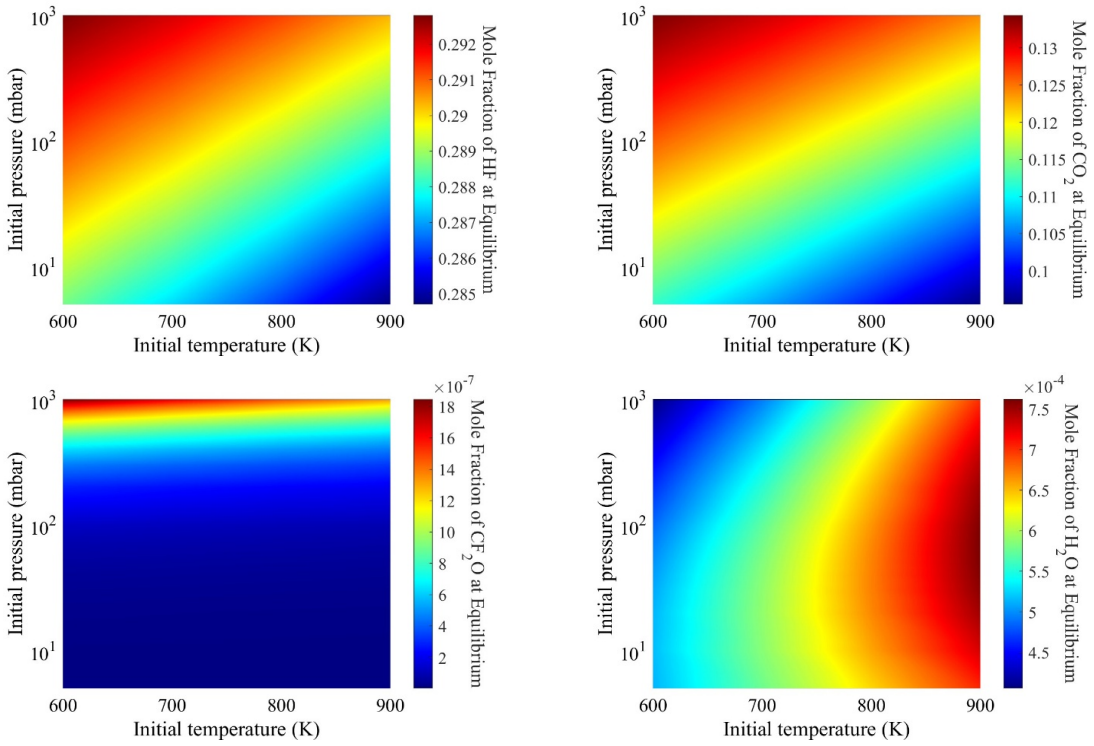

Fig. 1. Calculated mole fraction of CO_2, HF, CF_2O and H_2O for stoichiometric R32-air mixtures at equilibrium state.

that HF and CO_2 are two major products with relative high mole fractions at equilibrium state. The rest primarily consists of N_2, which acts as an inert gas in the system. Other species are present in low concentrations at equilibrium, as illustrated in Fig. 1 (lower), with CF_2O and H_2O shown as representative examples. Interestingly, unlike the combustion of hydrocarbon fuels where H_2O is a major product, H_2O is only an intermediate product in the combustion of R32. If combustion is complete, it exists at a very low concentration in chemical equilibrium.

Product CO_2 is one primary product, and its formation via CF_2O is a slow process [17, 18]. Besides that, CF_2O is a by-product, which can also be produced during the R32 combustion. CF_2O is highly toxic with a recommended exposure limit of only 2 ppm in average over 8 h, making it crucial for both process and environmental safety [19, 20].

The other major product HF is also highly toxic [13], and the Emergency Response Planning Guidelines (ERPGs) [21, 20], issued by the Ammerical Industrial Hygiene Association (AIHA), provides strict guideline for the handling of HF. For example, the ERPG-3 level for Hydrogen Fluoride (HF) at 50 ppm represents the concentration above which exposure for up to 1 h could cause life-threatening health effects or death.

2.3. Reactions at the wall surface

In the present work, seven global recombination/destruction reactions of reactive molecules on the surface are considered:

$$HO_2 \xrightarrow{wall} 0.5H_2O + 0.75O_2 \quad (S1)$$

$$O \xrightarrow{wall} 0.5O_2 \quad (S2)$$

$$H \xrightarrow{wall} 0.5H_2 \quad (S3)$$

$$OH \xrightarrow{wall} 0.5H_2O + 0.25O_2 \quad (S4)$$

$$H_2O_2 \xrightarrow{wall} H_2O + 0.5O_2 \quad (S5)$$

$$H + F \xrightarrow{wall} HF \quad (S6)$$

$$CHFO \xrightarrow{wall} HF + CO \quad (S7)$$

The first five surface reactions are the same as those used in [14]. Reactions (S6) and (S7) are two additional surface reactions considered for the destruction of fluoride-involving species. Radicals such as C_2HF, CFCO, and many other reactive species are not included in the modeling of surface reactions because it was shown by the calculations that they are present only in low concentrations (mole fractions in the order of magnitude or less than $O(10^{-6})$) and have a minor influence on the system dynamics. The efficiency of destruction of radicals at the wall surface due to these surface reactions is quantified by the destruction efficiency γ. Without any specification, $\gamma = 1 \cdot 10^{-3}$ is used for all surface reactions. For more details related to the modeling of surface reactions, readers can referred to [14].

It should be emphasized that other potential surface reactions, such as $H_2O + F \xrightarrow{wall} HF + OH$, can also be considered in this context. However, as will be shown later, the formation of HF is not primarily controlled by wall surface destruction processes involving F atoms. Furthermore, additional calculations including the heterogeneous hydrolysis of CF_2O with adsorbed water at the wall surface also showed only a minor influence on HF formation for the configurations considered in the present study.

Consequently, we have focused on a limited set of surface reactions in our analysis. It is important to note that these reaction pathways may become relevant under different operating conditions and will be investigated in future work.

2.4. Computational software

The in-house INSFLA code is used to solve the above mentioned governing equations using the finite difference method. The discretized governing equations are formulated as differential-algebraic equations, which are solved numerically using the LIMEX solver [22, 23]. The LIMEX solver handles the system of ordinary differential and algebraic equations resulting from the discretization, including control over integration time steps, enabling long-time integration with a minimal computational cost [22].

3. A priori discussion on non-explosion and explosion behaviors of the system

Typically, the auto-ignition process can be divided into two modes: a slow reaction phase (no explosion) and a rapid reaction phase leading to a successful auto-ignition [14, 24]. In this section, we will discuss the spatio-temporal thermo-kinetic states to discuss how both failed and successful explosions can occur under similar conditions with slight difference on temperatures. Throughout our study, we monitor the reaction process over a duration of 60 min (1 h). This time frame is consistent with

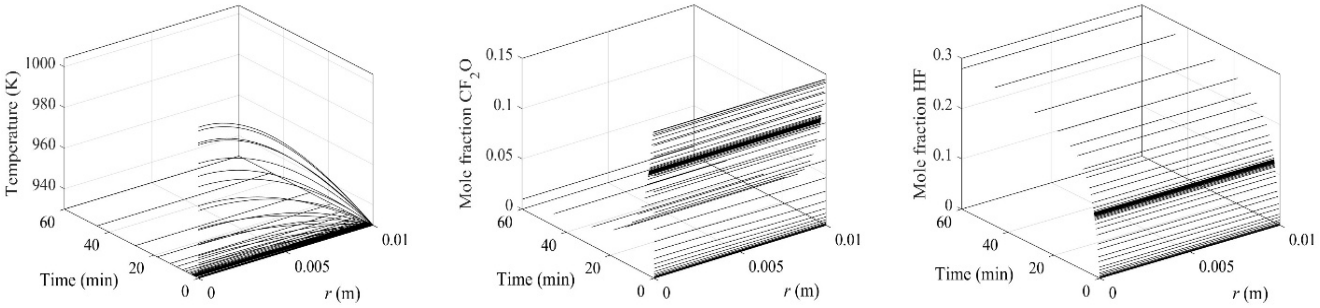

Fig. 2. Temporal-spatio development for a process with slow reaction. Conditions: T_0 = 930 K, p = 800 mbar, D = 20 mm, Φ = 1.0.

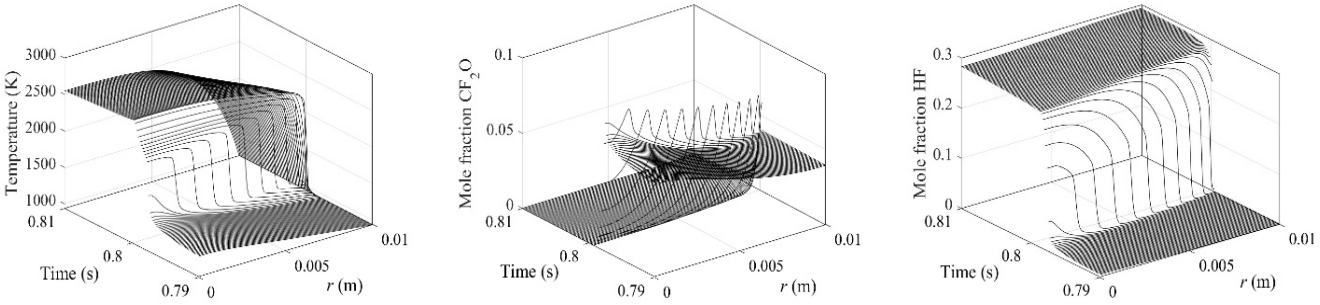

Fig. 3. Temporal-spatio development for a successful explosion. Conditions: T_0 = 940 K, p = 800 mbar, D = 20 mm, Φ = 1.0. The time axis is zoomed in on the region with significant state changes.

the guidelines outlined by the ERPG [21, 20], which specify that preventive actions must be taken within this period to reduce risks to human life.

Figure 2 illustrates an example of a slow reaction (no explosion) for T_0 = 930 K and p = 800 mbar, which is below the explosion limit. In addition to temperature, the mole fractions of CF_2O and CO_2 are chosen as representative species. It is observed that the temperature over the entire domain increases slightly by approximately 40 K before decreasing due to heat loss towards the vessel wall. However, despite the minor temperature increase, a certain amount of the highly toxic CF_2O is still formed (in this example, reaching a maximum mole fraction of around 15%). After reaching its maximum, the concentration of CF_2O begins to decrease. However, HF continues to be produced in high concentrations, even though the temperature changes only slightly. This is particularly interesting because, despite the absence of an explosion, the slow chemical reactions can still lead to the formation of toxic products like HF, which poses significant risks to human health and the environment. This indicates the importance of monitoring and controlling slow reaction processes, which may not show dramatic thermal changes but can still produce hazardous products or byproducts over time.

Figure 3 illustrates a typical example of a successful explosion for conditions where T_0 = 940 K and p = 800 mbar, whose temperature is slightly higher than the case in Fig. 2. In contrast to the slow reaction process shown above (c.f. Fig. 2), a successful explosion shows a sharp transition from slow reaction (characterized by moderate temperature rise) to ignition, characterized by an immediate temperature rise at the center of the vessel. Following the formation of the flame at the vessel center, the flame propagates outward. Concerning the HF species, it is also produced sharply during the explosion. Thus, explosion in all cases corresponds to an ignition in the center followed by a rapid flame propagation.

To illustrate this point further, Fig. 4 shows the time-dependent maximum temperature, pressure and mole fractions of CO_2 and HF for slow reactions (no explosions) with initial temperatures T_0 = 920 K (blue dashed lines) and T_0 = 930 K (red dashed line), and for successful explosions with initial temperatures T_0 = 940 K (yellow solid line) and T_0 = 950 K (purple solid line). It is clearly observed that for a

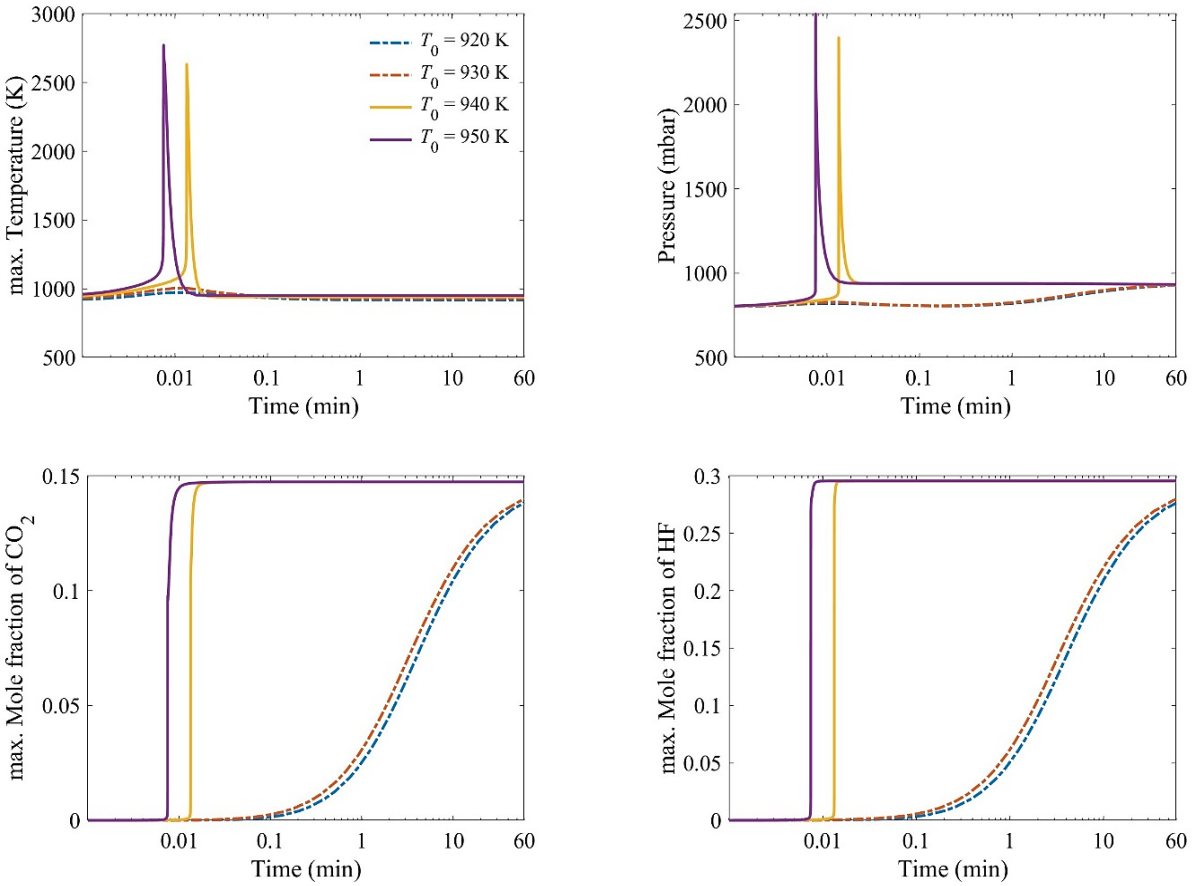

Fig. 4. Transient processes of different thermo-kinetic quantities with different initial temperatures T_0. Conditions: p = 800 mbar, D = 20 mm, Φ = 1.0.

successful explosion, a sharp temperature increase occurs for both initial temperature conditions, and the timing of this sharp temperature rise differs depending on the initial temperature. In contrast, for processes dominated by slow reactions, no sharp change in temperature is observed. Instead, the temperature increases gradually, with only mild variations over time. Regarding the main products, CO_2 and HF, it is observed that they are produced in relatively high concentrations. Their production rates, however, are strongly dependent on the initial temperatures. At higher initial temperatures, the reaction rates accelerate significantly, resulting in a rapid accumulation of these products. Conversely, at lower initial temperatures, the chemical reactions progress more slowly, leading to a gradual formation of CO_2 and HF over time. This indicates that even slow production at lower temperatures cannot be ignored, as the toxic HF is still produced to a large amount, which could present serious health and environmental concerns.

4. Results and Discussion

As seen above, in the case of slow reactions, although temperature changes may be slight and explosions are not observed, the production of toxic products such as HF can increase significantly over time. Thus, we can investigate the potential production of the toxic product HF even in the absence of an explosion. Therefore, in Fig. 5 different calculated initial temperatures and initial pressures are applied to show the maximum of temperature increase (left) and the maximum of HF production (right) within 60 min for R32-air mixtures with D = 20 mm. The vessel diameter of 20 mm is selected here to reflect the characteristic scales of typical refrigerant piping size. A surface destruction efficiency $\gamma = 1 \cdot 10^{-3}$ is used for all surface reactions at the wall (c.f. Section 2.3) in this figure. It is observed that within the considered temperature range (600–900 K), the maximum temperature increase reaches no more than 45 K. This indicates that, under all the initial temperature and pressure conditions shown, no sharp temperature rise associated with an explosion is observed.

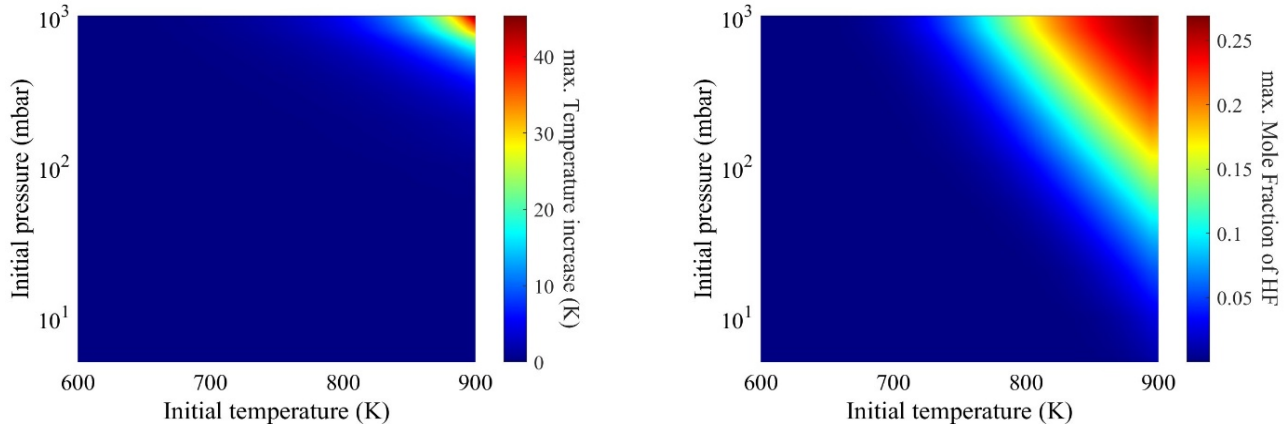

Fig. 5. Calculated maximum of temperature increase (left) and the production of HF (right) within 60 min for R32-air mixtures with D = 20 mm under different initial temperatures and initial pressures. Surface destruction efficiency $\gamma = 1{\cdot}10^{-3}$ is used for all surface reactions at the wall.

However, even with such low temperature increase, high amount of toxic HF can be produced. For sufficiently high initial temperatures, the maximum mole fraction of HF can reach approximately 25%, representing a significant concentration that results in a serious danger to human life. Performing a reaction pathway analysis, it is found that the dominant reaction step producing hydrogen fluoride (HF) is via the hydrolysis reaction step in the gas phase

$$CF_2O + H_2O \rightarrow CO_2 + 2HF,$$

and H_2O is produced mainly due to the hydrogen abstraction by OH of the CH_2F_2 in gas phase via:

$$CH_2F_2 + OH \rightarrow CHF_2 + H_2O.$$

This means that in the presence of OH radicals, H_2O will be produced, which serves as a precursor to produce HF.

Furthermore, it is worth investigating whether the production of HF is also sensitive to the surface reactions at the wall. In this case, the surface destruction efficiency γ of one surface reaction was varied between $\gamma = 1{\cdot}10^{-5}$ and $\gamma = 1{\cdot}10^{-2}$, while the surface destruction efficiency for all other surface reactions was kept at $\gamma = 1{\cdot}10^{-3}$. This range covers typical literature values reported for heterogeneous radical destruction on quartz and metal surfaces, including the relatively high decay probabilities of F atoms at the wall surface [25]. In Fig. 6, two initial conditions are presented as representative examples: the left one is for p = 20 mbar, T_0 = 784.6 K, and the right one is for p = 1000 mbar, T_0 = 623.2 K. The corresponding initial conditions ensure that the HF concentration after 60 min reaches the ERPG-3 level (50 ppm) if a surface destruction efficiency of $\gamma = 1{\cdot}10^{-3}$ is used for all surface reactions (c.f. Fig. 5).

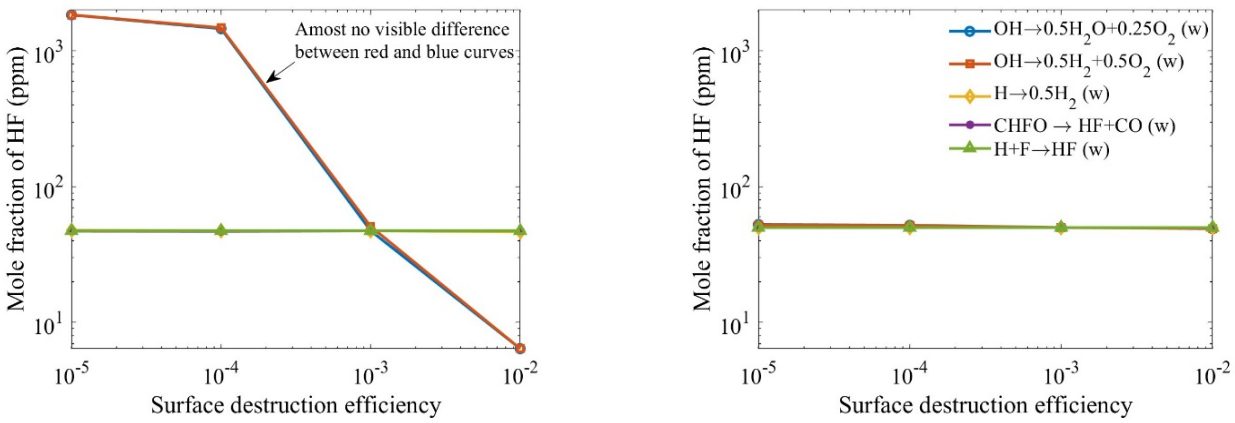

Fig. 6. Dependence of HF concentration on varying surface destruction efficiency γ of different surface reactions at the wall after 60 min. One color curve corresponds to the result by changing the surface destruction efficiency of one surface reaction, while keeping the surface destruction efficiency $\gamma = 1{\cdot}10^{-3}$ for all other surface reactions.

It is observed that, except for OH, the destruction of all other species at the wall surface (H, F, and CHFO in this figure; HO_2, O, H_2O_2 not shown here) plays only a minor role in the production of HF. The variation in surface destruction efficiency for all corresponding wall surface reactions has a negligible influence on the HF concentration. Furthermore, the destruction of OH at the wall surface plays a significant role in determining the HF concentration. While the change in HF concentration due to the variation in OH surface destruction efficiency at high pressure (in this figure, p = 1000 mbar) is only around 8%, it can vary by two orders of magnitude O(10^2) at low pressure (in this figure, p = 20 mbar). At elevated pressures, the chemical reaction rates become sufficiently fast such that the rate of the overall process is no longer mainly controlled by chemical kinetics, but rather by the transport of reactive species and energy. In particular, the transport of OH radicals toward the wall becomes the limiting process. As a consequence, variations in the surface destruction efficiency have only a minor influence on the overall OH consumption and therefore on HF formation.

Reaction pathway analysis shows that the variation is attributed to two competing reactions for the consumption of OH radicals:

$$CH_2F_2 + OH \rightarrow CHF_2 + H_2O.$$

$$OH \xrightarrow{\text{wall}} 0.5H_2O + 0.25O_2 \quad \text{or}$$

$$OH \xrightarrow{\text{wall}} 0.5H_2 + 0.5O_2$$

To produce HF, the OH radical is consumed through a reaction with CH_2F_2, resulting in the formation of H_2O, which is then further consumed in the subsequent hydrolysis step: ($CF_2O + H_2O \rightarrow CO_2 + 2HF$). This sequence of reactions emphasizes the crucial role of OH radicals in the production of HF. At lower pressures, the diffusive transport becomes faster, allowing OH radicals to reach the wall surface more readily where they are destroyed. This loss of OH radicals at the wall becomes significant because it reduces the availability of OH in the gas phase for the reaction with CH_2F_2. Consequently, the production of HF is directly impacted by the efficiency of OH radical destruction at the surface. This also explains why in Fig. 6 the HF concentration decreases with increasing surface destruction efficiency γ. As surface destruction efficiency increases, more OH radicals are destroyed at the wall surface, and a lowered conversion of CH_2F_2 into HF is expected.

Thirdly, it is interesting to note that the specific mechanism by which OH radicals are destroyed at the wall surface is less critical. What is essential is that the surface destruction of OH radicals must be included in the modeling of ignition process in the R32/air system to effectively capture the production of HF. This indicates that, regardless of the detailed pathways or reactions involved in the destruction process at the surface, accounting for this interaction provides critical insights into HF production.

In summary, the production of HF is closely linked to the presence of H_2O, which originates from OH radicals. These OH radicals play a dual role in the system: they can either react to form H_2O, thereby promoting HF production, or be consumed at the wall surface, effectively suppressing HF formation. This balance between the utilization and surface consumption of OH radicals significantly influences the overall HF yield in the system.

Figure 7 presents the calculated initial pressure-temperature conditions under which HF concentration reaches the ERPG-1, ERPG-2 and ERPG-3 threshold levels within 60 min for stoichiometric R32-air mixtures. These curves provide an overview of the thermo-kinetic conditions under which hazardous HF concentrations may develop, even in the absence of explosion (c.f. Fig. 5). It is clearly seen that the required initial temperature for reaching a given ERPG threshold increases significantly as the initial pressure decreases. At low pressures, higher initial

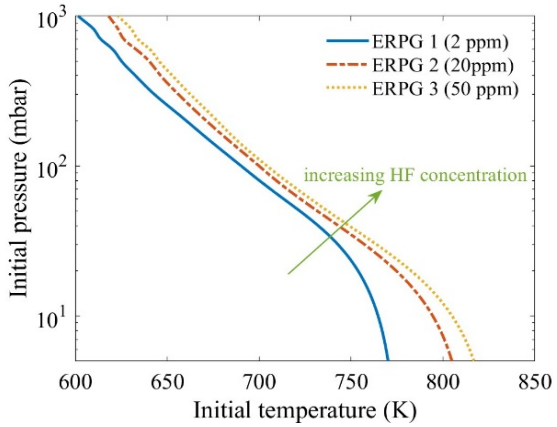

Fig. 7. Calculated initial pressure-temperature conditions corresponding to the ERPG threshold concentrations of HF after 60 min for stoichiometric R32-air mixtures with D = 20 mm and Φ = 1.0. The solid blue, dashed red and dotted yellow curves represent the initial conditions leading to the ERPG-1 (2 ppm), ERPG-2 (20 ppm) and ERPG-3 (50 ppm) HF concentration limits respectively. Surface destruction efficiency of $\gamma = 1 \cdot 10^{-3}$ are applied for all heterogeneous wall reactions.

temperatures are necessary to produce HF. In contract, at elevated pressures, hazardous HF concentrations can already be reached at relative lower initial temperatures due to accelerated reaction kinetics.

The figure further shows that the transition between different ERPG levels is relatively moderate compared to the overall pressure dependence. For example, under low-pressure conditions, an increase of only several tens of Kelvin can shift the system from ERPG-1 to ERPG-3 conditions. This indicates a strong sensitivity of HF formation to the initial thermo-kinetic state of the mixture.

5. Conclusion

This work numerically investigated the formation of toxic hydrogen fluoride (HF) during the auto-ignition process of stoichiometric R32-air mixtures under the influence of heat losses and heterogeneous wall reactions. Particular attention was paid to the production of HF under both slow reaction conditions and successful explosion scenarios.

The results show that significant amounts of HF can be produced even in the absence of explosion or significant temperature rise. Although slow reactions are characterized by only moderate thermal changes, they can still lead to continuous HF accumulation over extended times. This result suggests that non-explosion conditions in R32-air systems cannot necessarily be regarded as safe from a toxicological point of view.

Reaction pathway analysis showed that HF formation is mainly governed by the hydrolysis reaction of CF_2O with H_2O, while the required H_2O is primarily generated through OH-related reactions. Consequently, OH radicals play a key role in the overall HF production mechanism. Among all considered heterogeneous surface reactions, the destruction of OH radicals was found to have the strongest influence on HF formation, particularly at low pressures where diffusion molecular transport toward the wall becomes more important.

Furthermore, the calculated ERPG-based pressure-temperature limits indicate that hazardous HF concentrations can be reached within one hour over a wide range of non-explosion conditions. Such results indicate the importance of considering toxic product formation, in addition to explosion limits, when assessing the safety of R32-containing systems.

Finally, it should be noted that the employed chemical mechanism has not yet been validated against ignition delay time measurements due to the lack of available experimental data. Therefore, the present work mainly provided qualitative insights into the thermo-kinetic behavior and HF formation mechanisms in R32-air auto-ignition processes. Further work will focus on mechanism validation and quantitative analysis once suitable ignition delay measurements become available and updated chemical mechanisms are generated.

Finally, the authors want to emphasize that, due to the limited availability of detailed kinetics for R32, our analysis is constrained by the existing mechanism used in this work. A more accurate and comprehensive analysis will be conducted as soon as new validated mechanisms become accessible.

Acknowledgments

The authors gratefully acknowledge the financial contribution from the Deutsche Forschungsgemeinschaft (DFG) under the project FOR 5507, project number 497007546.

References

[1]. J. Calm, The next generation of refrigerants-Historical review, considerations, and outlook, *Int. J. Refrig.* 31 (2008) 1123–1133. DOI: 10.1016/j.ijrefrig.2008.01.013

[2]. P. Domanski, M. McLinden, Updating the limited options for low-global-warming-potential refrigerants, *Int. J. Refrig.* 178 (2025) 410–417. DOI: 10.1016/j.ijrefrig.2025.07.011

[3]. Y. Xu, L. Jia, Y. Ye, J. Liu, X. Shen, X. Han, Refrigerants evaluation and energy performance optimization for a high-temperature carbon dioxide+ hydrofluoroolefin/hydrochlorofluoroolefin cascade heat pump dryer with two air heating circuits, *Energy Convers. Manage.* 330 (2025) 119677. DOI: 10.1016/j.enconman.2025.119677

[4]. N. Kumma, S.H. Kruthiventi, Current status of refrigerants used in domestic applications: A review, *Renew. Sustain. Energy Rev.* 189 (2024) 114073. DOI: 10.1016/j.rser.2023.114073

[5]. M. Lee, S. Lee, J. Chung, S. Kwon, Y. Kim, Energy and environmental performances of heat pumps using R32 and R466A as alternatives to R410A, *Appl. Therm. Eng*. 256 (2024) 124140. DOI: 10.1016/j.applthermaleng.2024.124140

[6]. A. Mota-Babiloni, J. Navarro-Esbri, P. Makhnatch, F. Moles, Refrigerant R32 as lower GWP working fluid in residential air conditioning systems in Europe and the USA, *Renew. Sustain. Energy Rev.* 80 (2017) 1031–1042. DOI: 10.1016/j.rser.2017.05.216

[7]. Z. Yang, B. Feng, H. Ma, L. Zhang, C. Duan, et al., Analysis of lower GWP and flammable alternative refrigerants, *Int. J. Refrig.* 26 (2021) 12–22. DOI: 10.1016/j.ijrefrig.2021.01.022

[8]. J. Li, Z. Yang, H. He, C. Zhang, S. Hao, Research on the flammability and explosion characteristics of typical low GWP refrigerants, *J. Loss Prev. Process Ind.* 80 (2022) 104923. DOI: 10.1016/j.jlp.2022.104923

[9]. D. Burgess Jr, R. Burrell, V. Babushok, J. Manion, M. Hegetschweiler, G. Linteris, Burning velocity of R-32/O2/N2 mixtures: Experimental measurements and development of a validated detailed chemical kinetic model, *Combust. Flame* 236 (2022) 111795. DOI: 10.1016/j.combustflame.2021.111795

[10]. M. Hegetschweiler, J. Pagliaro, L. Berger, R. Hesse, J. Beeckmann, et al., Data reduction considerations for spherical R-32 (CH2F2)-air flame experiments, *Combust. Flame* 237 (2022) 111806. DOI: 10.1016/j.combustflame.2021.111806

[11]. T. Imamura, T. Sano, K. Yuzawa, O. Sugawa, Experimental evaluation of the possibility of ignition and flame propagation in accumulated difluoromethane (R32) from a kerosene cigarette lighter, *Loss Prev. Process Ind.* 43 (2016) 29–34. DOI: 10.1016/j.jlp.2016.04.003

[12]. K. Takizawa, N. Igarashi, K. Tokuhashi, S. Kondo, Effects of temperature and pressure on quenching distances of difluoromethane (R32) and ammonia (R717), *Sci. Technol. Built Environ.* 24 (2018) 97–104. DOI: 10.1080/23744731.2017.1328941

[13]. B. Feng, Z. Yang, R. Zhai, Experimental research on the concentration characteristics of R32 and R161 combustion product HF, *Energy* 125 (2017) 671–680. DOI: 10.1016/j.energy.2017.02.152

[14]. U. Maas, J. Warnatz, Ignition processes in hydrogen-oxygen mixtures, *Combust. Flame* 74 (1988) 53–69. DOI: 10.1016/0010-2180(88)90086-7

[15]. J. Hirschfelder, C. Curtiss, R. Bird, The molecular theory of gases and liquids, John Wiley & Sons, 1964.

[16]. V. Babushok, J. Donald, R. Kim, M. Hegetschweiler, G. Linteris, Modeling of combustion of fluorine-containing refrigerants, US Department of Commerce, National Institute of Standards and Technology, 2021. DOI: 10.6028/NIST.TN.2170

[17]. V. Babushok, G. Linteris, Kinetic mechanism of 2,3,3,3-tetrafluoropropene (HFO-1234yf) combustion, *J. Fluor. Chem*. 201 (2017) 15–18. DOI: 10.1016/j.jfluchem.2017.07.005

[18]. C. Needham, P. Westmoreland, Combustion and flammability chemistry for the refrigerant HFO-1234yf (2,3,3,3-tetrafluroropropene), *Combust. Flame* 184 (2017) 176–185. DOI: 10.1016/j.combustflame.2017.06.004

[19]. M. Farlow, E. Man, C. Tullock, R. Richardson. Carbonyl fluoride, *Inorg. Synth*. 6 (1960) 155–158. DOI: 10.1002/9780470132371.ch48

[20]. NIOSH, NIOSH pocket guide to chemical hazards, National Institute for Occupational Safety and Health, pp. 90-117, 1990.

[21]. F. Cavender, Emergency Response Planning Guidelines (ERPGs). Inhalation Toxicology, Inhalation Toxicology, CRC Press, Taylor and Francis Group, 2006, pp. 61–72. DOI: 10.1201/9781420037302.ch3

[22]. P. Deuflhard, U. Nowak, Extrapolation integrators for quasilinear implicit odes, Large Scale Scientific Computing, Springer, 1987, pp. 37–50. DOI: 10.1007/978-1-4684-6754-3_3

[23]. P. Deuflhard, E. Hairer, J. Zugck, One-step and extrapolation methods for differential-algebraic systems, *Numer. Math*. 51 (1987) 501–516. DOI: 10.1007/BF01400352

[24]. A. Levy, Kinetics of the hydrogen–oxygen–methane system. I. Inhibition of the second explosion limit, *J. Phys. Chem.* 59 (1955) 721–727. DOI: 10.1021/j150530a010